

Direct manipulation of diffusion in colloidal glasses via controlled generation of quasi-particle-like defects

Yi-Di Wang,^{1,2,*} Chu Xiao^{1,*}, Anupam Kumar^{1,3}, Yun-Hong Shi,¹ Chun-Shing Lee,^{1,2} King-Cheong Lam,⁴ Man-Kin Fung,⁵ Chor-Hoi Chan^{1,2,4}, Yuen-Hong Tsang,² Bo Li,¹ Chi-Hang Lam^{2,†} and Cho-Tung Yip^{1,‡}

¹*School of Science, Harbin Institute of Technology (Shenzhen), Shenzhen 518055, China*

²*Department of Applied Physics, Hong Kong Polytechnic University, Hung Hom, Hong Kong, China*

³*Department of Physics, Indian Institute of Technology (Indian School of Mines) Dhanbad, India*

⁴*Division of Science, Engineering and Health Studies, The School of Professional Education and Executive Development, Hong Kong Polytechnic University, Hung Hom, Hong Kong, China*

⁵*School of Science and Technology, Hong Kong Metropolitan University, Yau Ma Tei, Hong Kong, China*



(Received 26 May 2024; accepted 23 October 2024; published 10 December 2024)

We experimentally manipulate the structural relaxation of colloidal glass at an atomistically controlled position. We focus a laser beam to eject a particle from the colloidal system. This creates a void that transforms rapidly into a mobile soft spot (quasivoid) composed of a few neighboring free-volume fragments. The transformation and subsequent motions of the quasivoid trigger a sequence of well-connected stringlike motions emanating precisely from the point of laser action with free volumes flowing along the string. Furthermore, the sequence can be terminated by the annihilation of the quasivoid. The observations are supported by molecular dynamics (MD) simulations.

DOI: [10.1103/PhysRevE.110.064603](https://doi.org/10.1103/PhysRevE.110.064603)

I. INTRODUCTION

Defects in materials are of broad and fundamental interest because they are relevant to many physical properties such as elasticity, plasticity, and heat capacity [1]. For crystalline materials, defects can be identified from the interruption in the periodic order. In contrast, glass is characterized by a disordered microstructure [2–4] in which conventional definitions of defects for crystals do not apply [5,6]. Highly localized defects in the form of voids of sizes comparable to the particles in glasses are in general few and have been suggested to show only weak correlations with particle rearrangements [7–9]. These have cast doubt over their importance to glassy dynamics. It has also been reported that dynamics in glass formers at deep supercooling are dominated by stringlike motions [10–15]. Structural features enabling stringlike motions are suggested to be elementary excitations in glasses [12]. The origin of stringlike motions is still controversial and they have not been generated in any controlled manner. On the other hand, by using machine learning, one can identify a structural feature called softness, which gauges the tendency of particles to rearrange [16–18]. The soft spots are suggested to be associated with a reduced local particle density but precise structural characteristics and detailed microscopic mechanisms of soft-spot dynamics are not well understood [5,18–21].

Recently, a microscopic feature referred to as quasivoid capable of inducing stringlike motions in colloidal glass has

been identified [22]. It was shown to dominate structural relaxation at deep supercooling. A quasivoid consists of neighboring free volumes of a total size comparable to that of a particle. It is transported along the strings it induces. A direct evidence of its relevance in glasses is the reversible conversion into a vacancy when moving across a glass-crystal interface [22]. The quasivoid picture is consistent with the notion of soft spots [16–18] and locally favored structures [17] because the free volumes comprising the quasivoids clearly impact the local particle packings. It is also consistent with a recent finding that locally averaged free volumes correlate with long-time particle rearrangements in glass-forming liquids [23]. In the cooperative free volume model, the rate a molecule moves a distance on the order of its own size is dependent on the cooperation of surrounding molecules to open up enough free space [24]. Observations of quasivoids have also been reported in simulations of repulsive particles [25]. Furthermore, models based on void-induced particle dynamics offer possible explanations for a number of enduring mysteries in glass, including a wide range of fragility [26] and Kovacs paradox [27]. Quasivoids can thus be a key structural feature in glassy dynamics. As with crystalline materials, by understanding the nature of the key structural feature of soft spots, we may be able to manipulate them for fundamental study and to motivate new glassy properties and applications. However, direct microscopic manipulation of individual quasivoid, soft spot or locally favored structure has not yet been reported.

II. EXPERIMENT RESULT

In this work, we directly create soft spots in colloidal glass in the form of quasivoids with optical tweezers in

*These two authors contributed equally to this work.

†Contact author: c.h.lam@polyu.edu.hk

‡Contact author: h0260416@hit.edu.cn

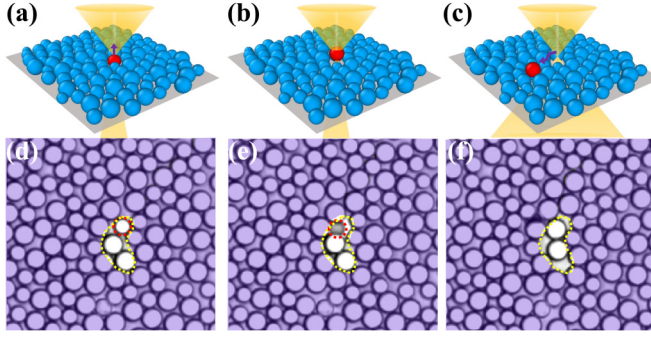


FIG. 1. Schematic diagrams and experimental time sequence of optical images of quasivoid formation by local laser tweezer. A beam focused slightly above a particle (red) exerts an upward force (a) which lifts the particle out of the 2D layer (b). It then diffuses away in the upper layer (c). In the experiment, a particle (red dotted line) is initially in the 2D layer (d). It is lifted, becoming out of focus (e), and then diffuses to a neighboring position in the upper layer (c). A region (yellow dotted line) initially contains three particles (d), (e) but finally holds only two and thus also one quasivoid (f).

experiments. We show that the as-created quasivoids dominate the subsequent dynamics. We also corroborate our findings in molecular dynamics (MD) simulations. In the experiments, we first prepare a 2D colloidal sample with a bimodal size mixture of polymethyl methacrylate (PMMA) spheres to suppress crystallization. The particles are immersed in water and confined between horizontal transparent glass plates. Most particles fall under gravity onto the lower plate forming a quasi-2D system with a packing fraction $\phi = 0.80$.

For colloidal crystals, point defects have been created by dragging individual particles from their lattice sites with optical tweezers [28,29]. However, for amorphous structures, such a process would significantly distort the particle arrangements in the local region. To solve this problem, instead of dragging it away, we find that it is possible to lift a particle to the upper layer with an optical tweezer. This creates a point defect in the form of a void that rapidly rearranges into a quasivoid with few other distortions in the further neighborhood. Specifically, we focus a pulsed laser beam (wavelength 1250 nm, repetition rate 1 KHz, and pulse width 30 fs) at a selected colloidal particle, as illustrated in Fig. 1(a). By maintaining the focal plane of the beam slightly above the particle, it can be lifted above the 2D layer [Fig. 1(b)]. It then diffuses away on the upper layer, leaving a void in the 2D layer [Fig. 1(c)].

An example of quasivoid creation is shown in Figs. 1(d)–1(f). Before laser illumination, all particles can be clearly imaged [Fig. 1(d)]. A particle to be grabbed by the laser tweezer is highlighted by a red dotted circle. When raised by the tweezer, it gets out of focus and appears dark and blurred [Fig. 1(e)]. We focused the laser on a particle using a light spot (diameter about 1.53 μm) smaller than the small particles (diameter 2.96 μm) so that it could tweeze only one particle. The contiguous free volume of size comparable to a particle is generated at the position of the lifted particle. Shortly after the departure of the lifted particle, a stringlike motion occurs, which transports and fragments the void into a few freevolumes which comprise a quasivoid [Figs. 2(a) and 2(b)]. After laser illumination, the region outlined by a yellow dotted

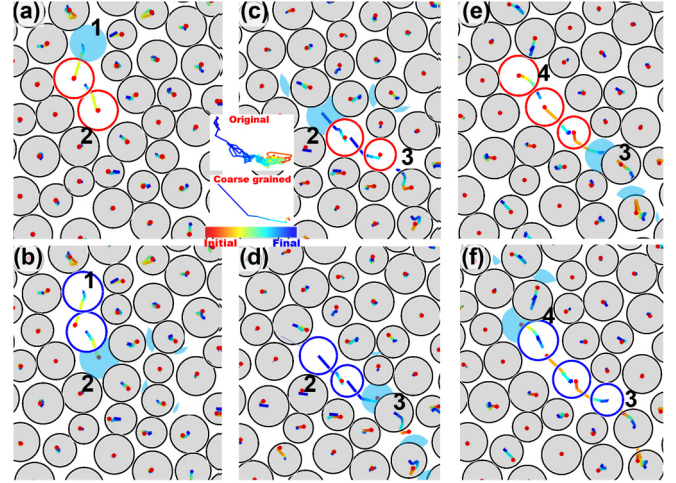


FIG. 2. Particle configurations during quasivoid formation. (a) and (b) show the same coarse-grained trajectories covering 20 s just after the particle ejection. Line segments in the trajectories are colored according to the times of occurrence. Initial positions are denoted by red dots. Particle configurations at the beginning (a) and the end (b) of the period are also shown. Inset: magnified views of the original and the coarse-grained trajectories of a typical hopped particle. Similarly, coarse-grained trajectories and initial/final configurations for the next 462 s and 1120 s are shown in (c), (d) and (e), (f) respectively. Blue areas show a void (a) and free-volume fragments constituting the quasivoid (b)–(f) as inferred from a push-off process associated with the stringlike motion.

line in Fig. 1(f) holds one less particle, as illustrated in Figs. 1(d)–1(f). Therefore, the region now possesses additional free volumes with a total size comparable to the ejected particle (See Ref. [30] for identifying these free volumes based on a push-off process). We have also observed similar quasivoid formation by directly removing a particle in MD simulations (MD simulations' result in Ref. [30]).

The as-created quasivoid instigates a sequence of four stringlike motions. Figure 2 shows the first two in detail and Fig. 3 shows the rest. In both figures, dynamics are illustrated using time-colored coarse-grained particle trajectories. Specifically, we first obtain the coarse-grained position $\mathbf{r}_i^c(t)$ of particle i at time t by averaging its instantaneous position $\mathbf{r}_i(t)$ over a coarsening time Δt_c :

$$\mathbf{r}_i^c(t) = \langle \mathbf{r}_i(t') \rangle_{t' \in [t, t + \Delta t_c]}. \quad (1)$$

The trajectory during time T_{traj} is plotted by joining every two consecutive positions $\mathbf{r}_i^c(t)$ and $\mathbf{r}_i^c(t + \Delta t_c)$ with a line segment colored according to t from red (initial time) to blue (final time) as shown in the inset in Fig. 2(c). These trajectories can illustrate the high mobility contrast among particles and hence also of the free volumes. The time-coloring enables the easy determination of the microstrings [31], i.e., strings or substrings in which all particles hop simultaneously as indicated by the same color of the dominant segment of the trajectory of each participating particle [22].

Figure 2(a) shows a string comprising two well-aligned trajectories of two particles ending up at position 1. Comparing the configurations before [Fig. 2(a)] and after [Fig. 2(b)] the

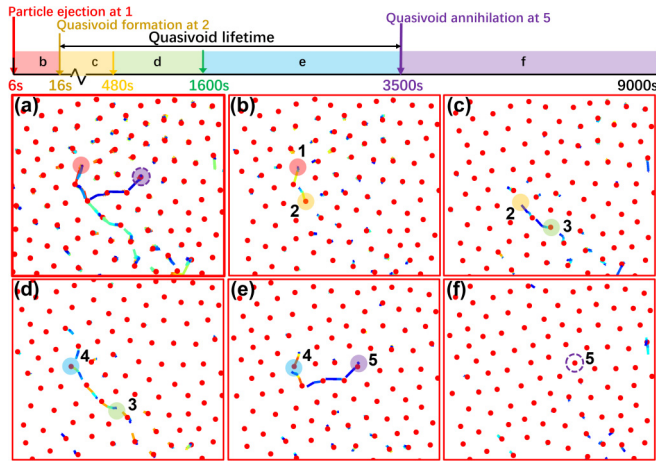


FIG. 3. Structural relaxation during the lifetime of a quasivoid. (a) Coarse-grained particle trajectories (colored lines) and their initial positions (red dots) covering a time of 9000 s. (b)–(f) Trajectories from (a) split up over consecutive time subintervals. A particle (red dotted circle) is then lifted to the upper layer by laser. A sequence of four stringlike motions is then observed (b)–(e). Numbered circles mark the initial and final positions of the quasivoids in the time subintervals. A particle from the upper layer then fills the quasivoid [purple dotted circles in (f)]. Particles become immobile again (f). The upper panel shows the timeline of events.

stringlike motion, we find that a contiguous void at position 1 is transported and fragmented into a few free volumes as indicated by the blue segments in Fig. 2(b). These fragments constitute a quasivoid at position 2. Remarkably, the quasivoid forms a metastable state without continual outward diffusion of its free volumes. Afterward, the quasivoid triggers another stringlike motion, which transports itself farther from position 2 to 3, where the fragmented volumes are transported from one local region to another over a distance determined by the string length as shown in Figs. 2(c) and 2(d). Then the quasivoid stays at position 3 for a while before relocating to position 4 via a stringlike motion shown in Figs. 2(e) and 2(f). Since in stringlike motions, all participating particles displace one another almost perfectly while nearby particles are practically stationary, a total free volume comparable to the typical particle size is transported in such motions [22]. Quasivoid motions are of strong back-and-forth nature and are far from diffusive at a short time. Other possible motions have also been suggested previously [32,33].

More interestingly, the quasivoid at position 4 continues to move by triggering further stringlike motions. Figure 3(a) shows the full dynamics over an extended period which covers the whole lifetime of the quasivoid. We observe a branched string connected precisely to where the quasivoid is created. This strongly supports the notion that stringlike motions are caused by quasivoids. Remarkably, the complex but well-aligned string structures show that the quasivoid survives a long sequence of transportation processes over a long duration. To examine the detailed dynamics, the same trajectories in Fig. 3(a) are broken down into time-consecutive sequences of trajectories as plotted in Figs. 3(b)–3(e). Figures 3(b) and 3(c) show again the first two stringlike motions depicted in

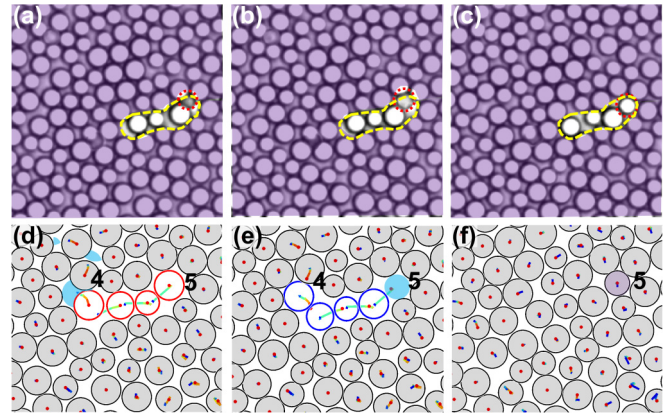


FIG. 4. Quasivoid annihilation by upper layer particle. A time sequence of optical images towards the end of the time interval depicted in Fig. 3(e). A particle (red dotted circle) is initially in the upper layer (a) and descends spontaneously to the 2D layer (b), (c). A region (yellow dotted line) initially contains three in-plane particles in (a), but finally holds four particles in (c). A quasivoid initially in the region is annihilated. (d)–(f) show the time sequence of the coarse-grained trajectories with particle configuration during the quasivoid annihilation process. The blue areas show that the quasivoid in (d) as inferred from the stringlike motion is transported into a void in (e) which is then annihilated by the upper layer particle (purple particle).

Figs. 2(c)–2(f). As shown in Figs. 3(d) and 3(e), two more stringlike motions then occur.

The whole sequence of particle trajectories realizing the stringlike motions in Figs. 3(b)–3(e) are well connected geometrically. More precisely, defining the direction of a string so that free volumes flow from a string tail to its head [22], the head of the preceding string coincides very well spatially with the tail of the subsequent one. The good connections can be easily understood from the step-by-step transport of the quasivoid from position 1 to 5. These motions are localized and highly intermittent, indicating the activated nature of quasivoid motions. The quasivoid thus also induces a whole mobile particle cluster formed by all the participants of stringlike motions. In contrast, particles not taking part in the stringlike motions are practically stationary. The mobile cluster in a background of stationary particles leads to dynamic heterogeneity typical of glass. Moreover, since the presence of quasivoids can be the main cause of soft spots, the transport of quasivoids via stringlike motions serves as a possible microscopic evolution mechanism of soft spots in colloidal glass.

After triggering the stringlike motions, we observe that the quasivoid is finally annihilated spontaneously by an upper-layer particle. Specifically, after a particle has hopped away from position 5 (purple dotted circle), as shown in Fig. 3(e), an extra particle abruptly emerges at the same position in Fig. 3(f). To show that the extra particle is from the upper layer, Fig. 4 shows a time sequence of optical images of the same region and coarse-grained trajectories with particle configuration during the annihilation. A particle is at a metastable position in the upper layer [red dotted circle in Fig. 4(a)]. It gradually lowers itself by pushing away neighboring particles

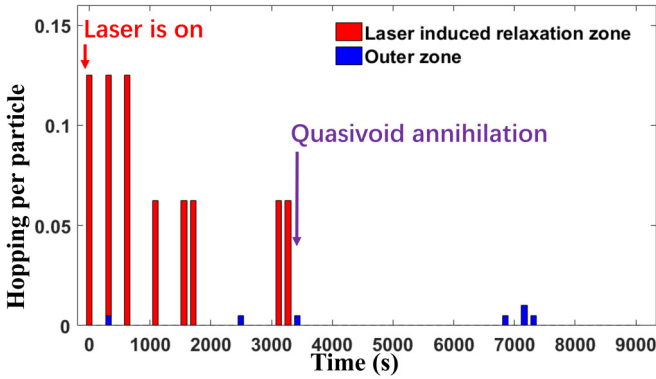


FIG. 5. Histogram of the number of hops per particle in 240 s in the region with laser-induced relaxation and its surrounding region for the same system in Fig. 2. The regions containing 30 and 90 particles, respectively, are defined in Fig. 7(c).

via a stringlike motion involving three particles [Figs. 4(a)–4(c)]. This transports the quasivoid from the left of a region marked by the yellow dotted line to the right. As demonstrated in the time sequence, the upper-layer particle finally fills the quasivoid and becomes fully incorporated into the 2D layer [Fig. 4(c)]. This annihilation of the quasivoid is also supported by the absence of further local relaxation in this region during even a long period of subsequent observation [Fig. 3(f)]. Therefore, by creating a quasivoid, we have generated stringlike structural relaxations which persist until the annihilation of the quasivoid by an upper-layer particle.

To illustrate quantitatively that additional relaxation has occurred during the lifetime of the quasivoid, Fig. 5 compares a histogram of the number of hops per particle in the laser-induced relaxation zone with that of an unaffected surrounding zone. In between the creation and annihilation of the quasivoid, particle hops are intermittent but are clearly more frequent in the laser-affected zone than elsewhere.

The experiment on quasivoid creation and annihilation is highly reproducible. More examples from similar experiments and MD simulations are reported in Ref. [30]. In all experiments, the ejection of a particle from the 2D layer is rapidly followed by a stringlike motion that also transforms the created void into a quasivoid. This indicates the high free energy of a contiguous void, which is lowered by fragmenting into a quasivoid due to its higher entropy. The transformation is associated with its movement from the tail to the head of the string as this may bring the quasivoid to a more energetically favorable location in the neighborhood. In the annihilation process, stringlike motions also closely precede the filling up of the quasivoids as the activation of these strings can be assisted by the presence of the upper layer particles.

III. MD RESULT

Next, we further verify these findings through MD simulations with extensive statistics. As shown in Fig. 6(a), a particle at position 1 is directly deleted to create a quasivoid. The generated quasivoid then initiates a sequence of stringlike motions, and at the same time, hopping from position 1 to 6. This is in line with observations from the colloidal experiments.

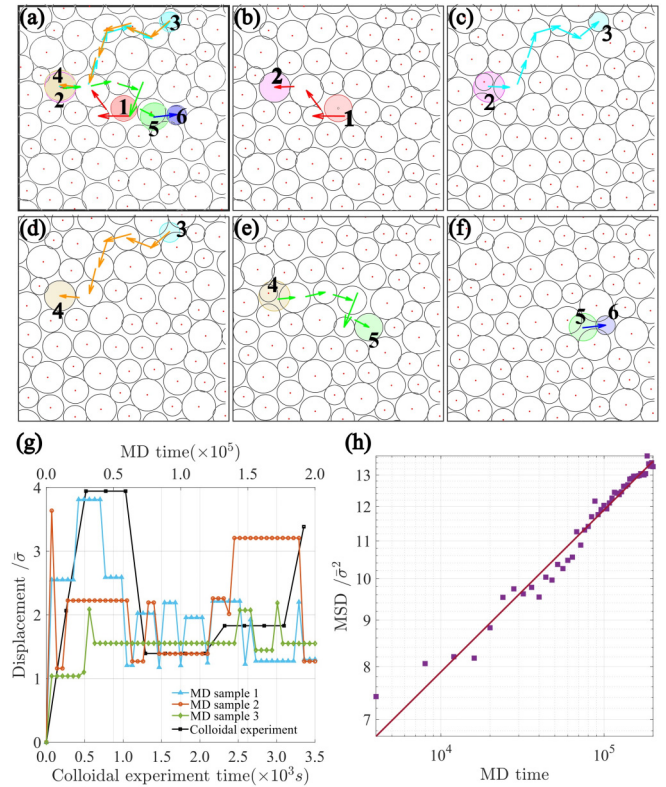


FIG. 6. Quasivoid dynamics. (a) Trajectory of quasivoid and initial particle configuration of MD sample 1 covering a duration of 2×10^5 . (b)–(f) Subtrajectories of the quasivoid covering consecutive time subintervals which constitute the full trajectory in (a). Arrows in trajectories show negative particle displacements, which indicate free-volume movements. Numbered circles denote the initial and final quasivoid positions of the time-subinterval. (g) Time-dependent displacement of quasivoids from a colloidal experiment and three representative MD simulations. (h) A log-log plot of quasivoid MSD averaged over 128 MD simulations (symbols) and a fit to a power law (line).

Figure 6(a) shows the overall trajectory of the quasivoid while Figs. 6(b)–6(f) illustrate the time sequence of subtrajectories that make up the overall trajectory. Detailed definitions and methodologies for locating quasivoid positions are provided in the Supplemental Material. The displacement of the quasivoid from its initial position can then be calculated. In contrast to random hopping motions of vacancies in the crystal [28], the quasivoid diffuses with numerous back-and-forth motions. We further obtain the mean square displacement (MSD) of the quasivoids averaged over 128 MD simulations [Fig. 6(h)]. The quasivoid MSD exhibits a subdiffusive behavior which is well-described by a power law relation

$$\text{MSD}/\bar{\sigma} = K_{\alpha} t^{\alpha}, \quad (2)$$

where the fitted exponent $\alpha = 0.18$ indicates a sublinear scaling with time t .

The quasivoids created by tweezers are indistinguishable from the intrinsic ones associated with spontaneous density fluctuations reported in Ref. [22], based on visual observations of particle configurations and geometries of particle trajectories they induce. They possess an excellent integrity

as implied by the long sequences of stringlike motions with good alignments from heads to tails. It is remarkable that the free-volume fragments do not easily disperse as one would expect in slight or moderate supercooling. This results from the inability of the individual fragments to activate particle hops and to be transported due to their small sizes.

The relevance of voids to glassy dynamics has been a controversial problem [7–9,34,35]. In this work, the removal of a particle primarily creates a contiguous void. Instead of remaining contiguous or dissolving completely, it rapidly transforms into a quasivoid with a lower free energy. Therefore, quasivoids rather than contiguous voids are more readily available intrinsically in glasses and can be the dynamically dominant form of voids. It also explains why previous studies, focusing essentially on contiguous voids, suggest only weak correlations of voids with particle rearrangements [7–9].

Stringlike motions have been suggested to dominate glassy dynamics [12,14,22]. Their origin is not well understood. Using laser tweezers, this work achieves the generation of stimulated stringlike motions at precisely controlled positions by creating quasivoids. This provides further evidence that voids and, in particular, quasivoids, induce stringlike motions as proposed in Ref. [22]. Adopting the picture that particle dynamics are induced by a sparse population of intrinsic voids, many phenomena of glass can be reproduced using lattice models [26,27,36] or analytic calculations [37].

The subdiffusive behavior of quasivoids in Eq. (2) results from the strong back-and-forth character of their motions as exemplified in Fig. 6(g). These features are in turn caused by the rugged potential energy landscape particles and thus quasivoids experience [38]. We have proposed [22] and further confirmed here that quasivoids facilitate particle motions. The subdiffusive relation in Eq. (2) hence should also explain a subdiffusive propagation of facilitated dynamics observed in simulated glassy systems [27,39].

Quasivoids in glasses are analogous to vacancies in crystals. The latter can be created via irradiation with energetic particles. Conversely, one can also fill in vacancies with small atoms, which suppresses diffusion and strengthens the crystal. Analogous to semiconductors in which electron holes can be created by doping, better controls of quasivoid creation and annihilation for glass formers in the future may enable new approaches for improving material properties.

IV. EXPERIMENTAL COLLOIDAL SYSTEMS

We use PMMA colloidal particles synthesized by microparticles GmbH for fabricating colloidal glass samples. To form a glassy state, we employ a bimodal (binary) mixture of these PMMA spheres to suppress crystallization. In this work, we use two solutions of small (s) and large (l) PMMA particles with average diameters $\sigma_1 = 2.96 \mu\text{m}$ and $\sigma_2 = 3.77 \mu\text{m}$, respectively, with number concentrations following a ratio of 0.55 : 0.45, as measured by the manufacturer. We use $\sigma = \sigma_1 = 2.96 \mu\text{m}$ as the basic length scale for data analysis. The diameter ratio of the big and small particles is $\sigma_2/\sigma_1 = 1.27$.

In all experiments, PMMA particles are immersed in water and confined between two horizontal transparent glass plates. The particles fall under gravity onto the lower glass plate forming quasi-two-dimensional (2D) systems. Only a very

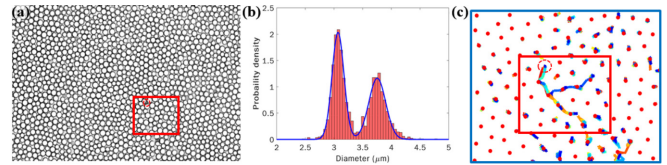


FIG. 7. Experimental results: (a) An optical image of a colloidal glass system formed by a bimodal mixture of PMMA particles. The number of particles within view is 1583. (b) Probability density function of particle diameters measured from the system in (a). The fitted function (blue curve) is the mixture of Gaussian with two components. (c) Coarse-grain particle trajectories in part of the system in (a) with 120 particles. (a) and (c) The region at which laser-induced relaxation occurs is indicated by a red box with 30 particles. A red dotted circle shows the position of the laser beam for optical tweezing.

small fraction of particles remains in an upper layer, and they do not noticeably perturb the 2D system unless they fall into the bottom layer. Digital videos are then recorded at a rate of one frame every 2 seconds using an optical microscope with an oil immersion objective (60X) and a CCD camera. The number of particles within an optical image is, for example, 1583 in a typical sample. All particles in the imaged region of the 2D layer are maintained within the depth of focus during the reported periods and all of them are successfully identified by image analysis software. Particle tracking is performed by image-processing codes from Ref. [40], which extract the positions of the centers of all imaged particles at different times. Focusing on equilibrated states, all measurements are performed after samples have been settled for at least one day.

An optical image of the glassy system is shown in Fig. 7(a). The region inside the red box corresponds to that shown in Figs. 2(d)–2(f). A red dotted circle marks the location of the focused laser beam used for ejecting a particle to the upper layer. Figure 7(b) shows the measured probability density function of the particle diameters.

The size of the ejected particle has a significant impact on triggering a stringlike motion and generating a mobile quasivoid. We have chosen to eject the small to medium-sized particles (diameters between about $2.8 \mu\text{m}$ and $3.3 \mu\text{m}$) in the colloid. Otherwise, if a small particle is ejected, the created free volumes can be too small to induce any motion. And, if a large particle is ejected, it may not diffuse more than one or two particle diameters away in the upper layer and will likely fall back into the void. We have recorded 33 events in which small to medium-sized particles were ejected, with 29 instances in which stringlike motions are observed. In the remaining four cases, the ejected particles are relatively small, but not necessarily the smallest ones. This lack of a sharp threshold is because the free volume originally present at the location of the ejected particle also plays a role in influencing the outcome. In contrast, we find experimentally that even a relatively small upper-layer particle can annihilate a quasivoid and terminate further local relaxation. In preparing our colloidal samples, we have adopted PMMA particles of an average size optimized for the quasivoid creation process. A large particle size reduces up-layer diffusion as already mentioned. If too small, creating the predominantly 2D layer

is challenging as multilayer systems are often obtained. The lifting of a particle also requires precisely focusing the laser above the particle for tweezer action. Untargeted laser illumination only results in increased particle vibrations without stringlike motion.

V. MOLECULAR DYNAMICS MODEL AND METHODS

MD simulations are conducted to further support the generality of the experimental results. All simulations are performed by using LAMMPS [41]. We study a 2D polydisperse repulsive system with $N = 4096$ particles, with which $N = 1024$ particles has been studied previously in Ref. [36]. The diameters of particles obey a uniform distribution in the range $D \in [0.6815, 1.3185]$ with a mean diameter $\bar{\sigma} = 1$. More precisely, we approximate the continuous distribution by a discrete one with 128 possible particle diameters for programming convenience. All simulations are executed by using the canonical ensemble (NVT) MD method. We impose periodic boundary conditions and a fixed simulation box size of 64×64 to maintain a particle number density $\rho = 1$. A repulsive potential and dimensionless units are used following Ref. [29]. The repulsive potential between particles with diameter σ_i and σ_j is written as

$$V_{ij} = v_0 \left(\frac{\sigma_{ij}}{r} \right)^{12}, \quad (3)$$

where r is the distance between two particles and

$$\sigma_{ij} = \frac{\sigma_i + \sigma_j}{2} (1 - \epsilon |\sigma_i - \sigma_j|), \quad (4)$$

where the nonadditive parameter ϵ is 0.2, which promotes intermixing of particles with large size differences. Using dimensionless units, model parameters $\bar{\sigma}$, m , and v_0 are all set to 1, where $\bar{\sigma}$, m , and v_0 are mean particle diameter, the mass of each particle, and unit of energy, respectively. To construct the initial simulation structure, each particle is assigned a type so that there is an equal number of particles in each type. Particle positions are randomly distributed onto a triangular lattice in the simulation box. Next, this system is equilibrated using a hybrid MD and swap Monte Carlo algorithm at temperature $T = 0.1$ during which the sample becomes amorphous. The time step for the Verlet integration is $\Delta = 0.001$, which is used for all simulations in this work.

To simulate the particle removal from a 2D layer by optical tweezers in the experiments, we randomly delete a particle from the equilibrium system. We then perform further MD simulations to study the quasivoid dynamics and the stringlike motions induced. Finally, we simulate the quasivoid annihilation by inserting a particle at the most recent quasivoid location, modeling the descent of an upper-layer particle to the 2D layer. To ensure successful insertion with minimal local stress, the inserted particle is set to be of the same size as the head particle of the last stringlike motion. The system is further simulated to demonstrate that no or few subsequent relaxations occur after the quasivoid annihilation.

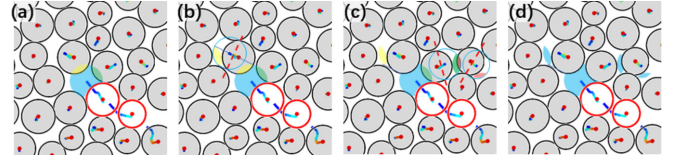


FIG. 8. (a)–(d) Coarse-grained trajectories showing a typical stringlike particle hopping motion from Fig. 2(f) in the main text. Particle configuration at the beginning of the time period is also shown. Red circles represent particles participating in the string with large displacements ($r_i^c > 0.8\sigma$). Free volumes (blue areas) constituting the invaded quasivoid are determined by successive push-off processes by the string tail particle based on mirror images of non empty regions (yellow, green, and purple areas) along the bisectors (red dotted lines) of the new and old positions of the pushed particles (b)–(c). The whole set of free volume fragments of quasivoid thus determined is shown in (d).

VI. IDENTIFICATION OF FREE-VOLUME FRAGMENTS COMPRISING A QUASIVOID

A quasivoid consists of a number of free volumes in a small neighborhood. We now suggest more systematic rules to define the free volumes based on a particle push-off process associated with a stringlike particle hopping motion. Defining the direction of a string according to the direction of free-volume transport and that a string points from its tail to head, a stringlike motion transports a quasivoid from its tail to head. Considering also that a particle hop corresponds to a displacement magnitude bigger than 0.8σ , the dip of the Van Hove correlation function, the last hopping particle in a string is referred to as the string head particle. We then define that a head particle directly invades a quasivoid during the stringlike motion. As Fig. 8(a) shows, the hopping particles (red circles) all have large displacements. The final occupied area of the tail particle was not completely free initially. Instead, it consists of a free volume (blue), which is the main fragment of the quasivoid, and two regions (yellow and green) initially occupied by two neighboring particles. During the stringlike motion, the two neighboring particles are pushed away, transporting free volumes in opposite directions for accommodating the tail particle. We thus locate the transported free-volume fragments in the following way: As shown in Fig. 8(b), we also draw the final position (blue open circle) of one of the pushed particles as well as a straight line (red dashed line) bisecting its initial and final positions. The yellow region is mirrored to the opposite side of the bisection line. The part of the mirrored region that is free [yellow region in Fig. 8(c)] is defined as another free-volume fragment of the quasivoid. The rest of the flipped region (green) is occupied by another neighboring particle. Considering similarly two further push-off and mirroring processes, we can identify two more free-volume fragments [green and red in Fig. 8(c)]. All these free-volume fragments of the quasivoid hence identified are shown in Fig. 8(d). Under this definition, the free volume fragments can be fitted together to regenerate the whole region invaded by the string tail (see Fig. 9).

We have found that the above rule-based definition of quasivoids generates reasonable geometries as the free-volume fragments of each determined quasivoid are closely clustered

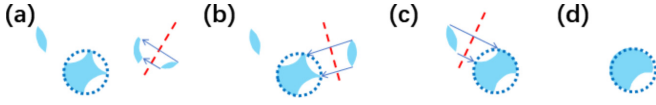


FIG. 9. Assembly of the quasivoid free-volumes. (a)–(c) Free-volume fragments of a quasivoid identified in Fig. 8 can be put together by the reversed mirroring process to generate the continuous free volume required by the hopping motion at the tail of the string.

within a few particle diameters and are clearly relevant to the particle hops. Noting the time-reversal symmetry of the dynamics in equilibrium supercooled liquids, the definition can similarly be applied to a quasivoid being vacated by the head particle of a string. In this definition, the quasivoid at a given position can be vacated and then invaded in two different consecutive stringlike motions and takes two different geometries. We have found that these geometries nevertheless share similar dominant free-volume fragments in general. Our definition of quasivoid geometry is by no means the only possible one. It is now based on the dynamics of quasivoids. It will be interesting to define quasivoids objectively in the future based only on the static structures.

VII. QUASIVOID TRAJECTORIES IN EXPERIMENTS AND SIMULATIONS

We trace a quasivoid trajectory by identifying a string of particle hopping motions during a time interval. The free volume comprising the quasivoid is transported from one end of the string to the other. At subsequent time intervals, the quasivoid can generate further stringlike motions to extend the quasivoid trajectory. The procedures are as follows:

(1) We first identify the initial quasivoid position $\mathbf{r}_q(t = 0)$. At $t = 0$, the quasivoid is situated at the previous position of the removed particle. As shown in Fig. 6, position 1 represents the initial quasivoid location.

(2) Identify particle hopping events. A hop at time $t = n\delta t$ ($n = 0, 1, 2, \dots$) is identified by: $|\mathbf{r}_i^c(t) - \mathbf{r}_i^c(t + \delta t)| \geq 0.6\bar{\sigma}$. Here, $\mathbf{r}_i^c(t)$ denotes the coarse-grained position at time t obtained by Eq. (1). The time interval δt we adopt in tracing quasivoid motion is larger than the coarsening duration Δt_c . To ensure the precise tracing of quasivoids, Δt_c is chosen to be sufficiently long to ensure particle vibrations are mostly averaged out while it is short enough to minimize the occurrence of hops during averaging.

(3) Determine quasivoid motion induced by particle hop. We examine sequentially time $t = n\delta t$. The quasivoid moves if particle i hops at time t and if its hopped position is close to the instantaneous position of the quasivoid, i.e.

$|\mathbf{r}_i^c(t + \delta t) - \mathbf{r}_q(t)| \leq 0.5\bar{\sigma}$. Then we define that the quasivoid is transported to the pre-hopped position of particle i , i.e. $\mathbf{r}_q(t + \delta t) = \mathbf{r}_i^c(t)$. Otherwise, the quasivoid's position is unchanged. Note that at any time t , the quasivoid can be transported stepwise by multiple hops in a stringlike motion.

For our experiments and MD simulations, we adopt $\delta t = 258$ s, $\Delta t_c = 178$ s, and $\delta t = 4000$ (dimensionless time), $\Delta t_c = 180$, respectively. The coarse-grained position is evaluated by averaging over 90 instantaneous positions captured every 2 seconds for colloidal experiments while 10 instantaneous positions captured every 20 time units are used for MD simulations. By following the procedures above, the quasivoid positions at different times can be obtained. The particle hops that contributed to the motions of the quasivoid are illustrated in Figs. 6(b)–6(f). Note that each hop is denoted nevertheless by the minus particle displacement (i.e., $-(\mathbf{r}_i^c(t + \Delta t_c) - \mathbf{r}_i^c(t))$), which indicates the direction of quasivoid motion.

In summary, we have demonstrated a way to generate dynamics-dominating local soft spots in the form of quasivoids in colloidal glass by ejecting particles from a 2D system with optical tweezers. By using digital video microscopy, we monitor particle dynamics during and after particle ejection. A void generated from the particle ejection process transforms into a quasivoid, which consists of fragmented free volumes. The quasivoid can be transported by the stringlike motions it induces. As indicated by the generation of a sequence of well-connected stringlike motions, a quasivoid survives multiple transportation steps that also result in a mobile particle cluster. The sequence of stringlike relaxations can be terminated by annihilating the quasivoid with an upper-layer particle. This demonstrates the possibility of manipulating local soft spots to modify glassy properties. Our findings will shed fresh light on the fundamental understanding of glass.

ACKNOWLEDGMENTS

We thank Hai-Yao Deng and Xiaoguang Ma for their helpful discussions. This work was supported by National Natural Science Foundation of China (Grants No. 2174079 and No. 12205066), Guangdong Basic and Applied Basic Research Foundation (Grants No. 2214050004792 and No. 2024A1515011775), Shenzhen Municipal Science and Technology projects (Grant No. JCYJ20200109113003946), General Research Fund of Hong Kong (Grant No. 15303220), Shenzhen Start-Up Research Funds (Grant No. BL20230925), Guangdong Provincial Key Laboratory of Semiconductor Optoelectronic Materials and Intelligent Photonic Systems, and Harbin Institute of Technology (Shenzhen, People's Republic of China).

- [1] D. Hull and D. J. Bacon, Origin and multiplication of dislocations, *Introduction to Dislocations*, 5th ed. (Butterworth-Heinemann, Oxford, UK, 2011), p. 157..
- [2] F. H. Stillinger and P. G. Debenedetti, Glass transition thermodynamics and kinetics, *Annu. Rev. Condens. Matter Phys.* **4**, 263 (2013).

- [3] G. Biroli and J. P. Garrahan, Perspective: The glass transition, *J. Chem. Phys.* **138**, 12A301 (2013).
- [4] F. Arceri, F. P. Landes, L. Berthier, and G. Biroli, Glasses and aging: A statistical mechanics perspective, [arXiv:2006.09725](https://arxiv.org/abs/2006.09725).
- [5] Z. Wang and W.-H. Wang, Flow units as dynamic defects in metallic glassy materials, *Natl. Sci. Rev.* **6**, 304 (2019).

- [6] A. Nicolas, E. E. Ferrero, K. Martens, and J.-L. Barrat, Deformation and flow of amorphous solids: Insights from elastoplastic models, *Rev. Mod. Phys.* **90**, 045006 (2018).
- [7] S. Swayamjyoti, J. F. Löffler, and P. M. Derlet, Local structural excitations in model glasses, *Phys. Rev. B* **89**, 224201 (2014).
- [8] J. Conrad, F. W. Starr, and D. Weitz, Weak correlations between local density and dynamics near the glass transition, *J. Phys. Chem. B* **109**, 21235 (2005).
- [9] A. Widmer-Cooper and P. Harrowell, Free volume cannot explain the spatial heterogeneity of debye-waller factors in a glass-forming binary alloy, *J. Non-Cryst. Solids* **352**, 5098 (2006).
- [10] H. Miyagawa, Y. Hiwatari, B. Bernu, and J. Hansen, Molecular dynamics study of binary soft-sphere mixtures: Jump motions of atoms in the glassy state, *J. Chem. Phys.* **88**, 3879 (1988).
- [11] C. Donati, J. F. Douglas, W. Kob, S. J. Plimpton, P. H. Poole, and S. C. Glotzer, Stringlike cooperative motion in a supercooled liquid, *Phys. Rev. Lett.* **80**, 2338 (1998).
- [12] A. S. Keys, L. O. Hedges, J. P. Garrahan, S. C. Glotzer, and D. Chandler, Excitations are localized and relaxation is hierarchical in glass-forming liquids, *Phys. Rev. X* **1**, 021013 (2011).
- [13] M. Isobe, A. S. Keys, D. Chandler, and J. P. Garrahan, Applicability of dynamic facilitation theory to binary hard disk systems, *Phys. Rev. Lett.* **117**, 145701 (2016).
- [14] C.-H. Lam, Repetition and pair-interaction of string-like hopping motions in glassy polymers, *J. Chem. Phys.* **146**, 244906 (2017).
- [15] Y. Sun, S.-X. Peng, Q. Yang, F. Zhang, M.-H. Yang, C.-Z. Wang, K.-M. Ho, and H.-B. Yu, Predicting complex relaxation processes in metallic glass, *Phys. Rev. Lett.* **123**, 105701 (2019).
- [16] E. D. Cubuk, R. Ivancic, S. S. Schoenholz, D. Strickland, A. Basu, Z. Davidson, J. Fontaine, J. L. Hor, Y.-R. Huang, Y. Jiang *et al.*, Structure-property relationships from universal signatures of plasticity in disordered solids, *Science* **358**, 1033 (2017).
- [17] C. P. Royall and S. R. Williams, The role of local structure in dynamical arrest, *Phys. Rep.* **560**, 1 (2015).
- [18] S. S. Schoenholz, E. D. Cubuk, D. M. Sussman, E. Kaxiras, and A. J. Liu, A structural approach to relaxation in glassy liquids, *Nat. Phys.* **12**, 469 (2016).
- [19] S. S. Schoenholz, A. J. Liu, R. A. Riggleman, and J. Rottler, Understanding plastic deformation in thermal glasses from single-soft-spot dynamics, *Phys. Rev. X* **4**, 031014 (2014).
- [20] E. Ma, Tuning order in disorder, *Nat. Mater.* **14**, 547 (2015).
- [21] X. Ma, Z. S. Davidson, T. Still, R. J. Ivancic, S. Schoenholz, A. Liu, and A. Yodh, Heterogeneous activation, local structure, and softness in supercooled colloidal liquids, *Phys. Rev. Lett.* **122**, 028001 (2019).
- [22] C.-T. Yip, M. Isobe, C.-H. Chan, S. Ren, K.-P. Wong, Q. Huo, C.-S. Lee, Y.-H. Tsang, Y. Han, and C.-H. Lam, Direct evidence of void-induced structural relaxations in colloidal glass formers, *Phys. Rev. Lett.* **125**, 258001 (2020).
- [23] B. Mei, B. Zhuang, Y. Lu, L. An, and Z.-G. Wang, Local-average free volume correlates with dynamics in glass formers, *J. Phys. Chem. Lett.* **13**, 3957 (2022).
- [24] R. P. White and J. E. Lipson, Explaining the T,V -dependent dynamics of glass forming liquids: The cooperative free volume model tested against new simulation results, *J. Chem. Phys.* **147**, 184503 (2017).
- [25] Y.-C. Hu and H. Tanaka, Origin of the boson peak in amorphous solids, *Nat. Phys.* **18**, 669 (2022).
- [26] C.-S. Lee, M. Lulli, L.-H. Zhang, H.-Y. Deng, and C.-H. Lam, Fragile glasses associated with a dramatic drop of entropy under supercooling, *Phys. Rev. Lett.* **125**, 265703 (2020).
- [27] M. Lulli, C.-S. Lee, H.-Y. Deng, C.-T. Yip, and C.-H. Lam, Spatial heterogeneities in structural temperature cause kovacs' expansion gap paradox in aging of glasses, *Phys. Rev. Lett.* **124**, 095501 (2020).
- [28] A. Pertsinidis and X. S. Ling, Equilibrium configurations and energetics of point defects in two-dimensional colloidal crystals, *Phys. Rev. Lett.* **87**, 098303 (2001).
- [29] A. Pertsinidis and X. Ling, Diffusion of point defects in two-dimensional colloidal crystals, *Nature (London)* **413**, 147 (2001).
- [30] See Supplemental Material at <http://link.aps.org/supplemental/10.1103/PhysRevE.110.064603> for more experiment details; identifying freevolumes based on a push-off process; md simulations' results; more examples from similar experiments and MD simulations.
- [31] Y. Gebremichael, M. Vogel, and S. C. Glotzer, Particle dynamics and the development of string-like motion in a simulated monoatomic supercooled liquid, *J. Chem. Phys.* **120**, 4415 (2004).
- [32] Q. Tang, W. Hu, and S. Napolitano, Slowing down of accelerated structural relaxation in ultrathin polymer films, *Phys. Rev. Lett.* **112**, 148306 (2014).
- [33] H. Tian, J. Luo, Q. Tang, H. Zha, R. D. Priestley, W. Hu, and B. Zuo, Intramolecular dynamic coupling slows surface relaxation of polymer glasses, *Nat. Commun.* **15**, 6082 (2024).
- [34] C.-H. Lam, Deeper penetration of surface effects on particle mobility than on hopping rate in glassy polymer films, *J. Chem. Phys.* **149**, 164909 (2018).
- [35] S. Napolitano and D. Cangialosi, Interfacial free volume and vitrification: Reduction in t_g in proximity of an adsorbing interface explained by the free volume holes diffusion model, *Macromolecules* **46**, 8051 (2013).
- [36] G. Gopinath, C.-S. Lee, X.-Y. Gao, X.-D. An, C.-H. Chan, C.-T. Yip, H.-Y. Deng, and C.-H. Lam, Diffusion-coefficient power laws and defect-driven glassy dynamics in swap acceleration, *Phys. Rev. Lett.* **129**, 168002 (2022).
- [37] H.-Y. Deng, C.-S. Lee, M. Lulli, L.-H. Zhang, and C.-H. Lam, Configuration-tree theoretical calculation of the mean-squared displacement of particles in glass formers, *J. Stat. Mech.: Theory Exp.* (2019) 094014.
- [38] C.-H. Lam, Local random configuration-tree theory for string repetition and facilitated dynamics of glass, *J. Stat. Mech.: Theory Exp.* (2018) 023301.
- [39] C. Scalliet, B. Guiselin, and L. Berthier, Thirty milliseconds in the life of a supercooled liquid, *Phys. Rev. X* **12**, 041028 (2022).
- [40] J. C. Crocker and E. R. Weeks, Particle tracking using IDL (2011), Retrieved from <https://physics.emory.edu/faculty/weeks/idl/>.
- [41] A. P. Thompson, H. M. Aktulga, R. Berger, D. S. Bolintineanu, W. M. Brown, P. S. Crozier, P. J. in't Veld, A. Kohlmeyer, S. G. Moore, T. D. Nguyen *et al.*, LAMMPS—a flexible simulation tool for particle-based materials modeling at the atomic, meso, and continuum scales, *Comput. Phys. Commun.* **271**, 108171 (2022).